

GEOMETRICALLY CONSTRAINED ICA FOR ROBUST SEPARATION OF SOUND MIXTURES

Mirko Knaak^{†‡} *Shoko Araki*[†] *Shoji Makino*[†]

[†] NTT Communication Science Laboratories, NTT Corporation
2-4 Hikaridai, Seika-cho, Soraku-gun, Kyoto 619-0237, Japan
e-mail: Mirko.Knaak@tu-berlin.de

[‡] Technical University Berlin, Measurement Technology Lab
Einsteinufer 19, 10587 Berlin, Germany

ABSTRACT

Based on the equivalence of blind source separation and adaptive beamforming, this paper introduces a new algorithm using independent component analysis with a geometrical constraint. The new algorithm solves the permutation problem of the blind source separation of acoustic mixtures, and is significantly less sensitive to the precision of the geometrical constraint than an adaptive beamformer. A high degree of robustness is very important since the steering vector is always roughly estimated in a reverberant environment, even when the look direction is precise. The new algorithm is based on FastICA and constrained optimization. It is theoretically and experimentally analyzed with respect to the roughness of the steering vector estimation by using impulse responses of a real room. The effectiveness of the algorithms for real-world mixtures is also shown for three sources and three microphones.

1. INTRODUCTION

For many signal processing tasks, such as speech recognition, transmission, or signals classification, a very good target signal reconstruction of the is essential when the target signal is disturbed by other sources. Adaptive beamformers (ABF) and blind source separation (BSS) are very effective tools for multichannel signal reconstruction.

Although the utility of ABFs is well established [1], they have limited robustness against erroneous parameters. This is problematic since the steering vector is always roughly estimated in a reverberant environment, as shown in this paper. The methods traditionally used to overcome this sensitivity mostly broaden the directivity pattern, resulting in a trade-off between the signal suppression performance and the parameter sensitivity (e.g., [2],[3]).

Independent component analysis ICA is an emerging technique for finding statistically independent components in a multi-channel signal. The main applica-

tion is BSS which has been shown to be capable of recovering multiple sources from their linear mixture if the sources are independent [4].

In the field of acoustics, convolutive mixtures need to be separated and this involves estimating many more parameters (see [5] for references) than when separating a scalar mixture. Most approaches simplify the problem into instantaneous separation problems for the frequency components (e.g., [6],[7]). The scaling and permutation ambiguities that remain in the recovered frequency components pose a serious problem, particularly when the number of sources and microphones becomes greater than two. Different frequency component permutations lead to mixed outputs and degraded separation results. There are several approaches to overcoming this problem (e.g., [8]) however, they are restricted to two sources. Hence, the number of real-world applications in the acoustics field is still very limited, and the separation performance is mostly insufficient [9].

Recent research has indicated an equivalence between ABF and BSS, e.g., [10],[11]. BSS is only an intelligent set of ABFs with an adaptive null directivity aimed in the direction of the unnecessary sounds, which have been employed by [12]. This equivalence suggests the application of a geometrical constraint to ICA to solve the permutation and scaling problem.

Geometrically constrained algorithms have been proposed by [13]-[15]. These contributions do not assess in detail how a rough estimation of the steering vector effects the performance of the algorithms. They only employ the constraint with the assumption that it is estimated correctly. This assumption is very limiting because precise information about the steering vector is very difficult to obtain. The major advantage of using ICA and geometrical information appears when only a rough estimation is possible. Furthermore, their algorithms are rather slow iteration type algorithms.

This paper proposes a new geometrically constrained ICA algorithm that employs the fast convergence prop-

erties of the FastICA algorithm [4]. We also analyze the behavior of geometrically constrained ICA algorithms in general with respect to a rough estimation of the constraint. In Sec. 2, we make basic assumptions on the mixture, ABF and BSS algorithms, and analyze the possible reasons for a rough estimation of the steering vector. The new algorithm is introduced and assessed theoretically and experimentally in Sec. 3.

2. BLIND SOURCE SEPARATION AND ADAPTIVE BEAMFORMERS

2.1. Signals and BSS algorithm

In a set $\mathbf{s}^b(t) = [s_{\text{target}}^b(t), s_{i1}^b(t), \dots, s_{iN-1}^b(t)]^T$ of broadband sources, the first source is the target sound and the others are interfering sources. The sound is measured with an array of M microphones $\mathbf{x}^b(t) = [x_1^b(t), \dots, x_M^b(t)]^T$. The observed signals are filtered and mixed because the room acoustics impose a different impulse response h_{mn}^b between each source s_n^b and each microphone x_m^b .

In the frequency domain, a convolutive mixture can be written as $\mathbf{x}^f = \mathbf{H}^f \cdot \mathbf{s}^f + \mathbf{n}^f$, where \mathbf{x}^f is a narrow-band signal component filtered from \mathbf{x}^b with a band-pass centered at f . For simplicity, the index f is omitted hereafter. $\mathbf{H} = [\mathbf{h}_1, \dots, \mathbf{h}_N]$ consists of the steering vectors \mathbf{h}_N , where \mathbf{h}_1 is the steering vector of the target sound. Only under anechoic conditions, they can be approximated by the phase shifts caused by the time delays τ_{mn} with $\mathbf{h}_n = [e^{j2\pi f \tau_{1n}}, \dots, e^{j2\pi f \tau_{Mn}}]^T$. When considering echoes and reverberation, \mathbf{h}_n is the sum of all echo paths.

The goal of the algorithms discussed here is to find an optimal estimation $y_1(t)$ of the target signal s_{target} . To achieve this goal, an unmixing matrix \mathbf{W} or a coefficient vector \mathbf{w}_1 is applied to the vector of observations as follows:

$$\mathbf{y} = \mathbf{W} \cdot \mathbf{x} \quad y_1 = \mathbf{w}_1^H \cdot \mathbf{x}, \quad (1)$$

where $\langle \rangle^H$ is the hermitian (conjugate transposed).

Blind source separation uses ICA to estimate the unmixing matrix $\mathbf{W} = [\mathbf{w}_1, \dots, \mathbf{w}_N]^H$ by making the output signals as independent as possible. Essentially, ICA has two steps ($\mathbf{W} = \mathbf{T}^H \cdot \mathbf{V}$). In the first step (sphering), the matrix \mathbf{V} is determined by principle component analysis (PCA). In the second step (rotation with \mathbf{T}), one can use maximization of nongaussianity, nonlinear decorrelation, non-stationary decorrelation, or spatio-temporal decorrelation to determine the rotation matrix \mathbf{T} [4].

2.2. ABF with an imprecise estimation of the steering vector

An ABF minimizes the power of the output signal with a constraint: the energy of a signal coming from the direction of the target is passed unchanged $\mathbf{w}_1^H \hat{\mathbf{h}}_1 = c_1$. This means that the source position has to be known in advance. It can be estimated by sound localization methods (e.g., MUSIC [1]), determined by image processing, or simply known by geometry.

A major drawback of ABFs is that they rely on the correct estimation of the steering vector. Since the impulse response of a room is normally not available, the steering vector $\hat{\mathbf{h}}_1$ is estimated solely from the time delays of the direct sound. An estimation error of $\hat{\mathbf{h}}_1$ has two causes: a wrong direction of arrival, or the existence of strong reverberations. The latter cause is due to the multiple directions of arrival while only the direct sound is used for the estimation. The estimation becomes rough even when the source position is well known.

To determine the error made by a rough estimation of $\hat{\mathbf{h}}_1$, we introduce a new measure: the steering vector error angle (SVA) μ . For its definition, we use a generalized cosine $\cos(\mathbf{x}, \mathbf{y}) = |\mathbf{x}^H \mathbf{y}| / |\mathbf{x}| |\mathbf{y}|$ to define the angle between two complex vectors \mathbf{x} and \mathbf{y} . Let $\mu(f)$ be the angle between $\hat{\mathbf{h}}_1(f)$ and $\mathbf{h}_1(f)$ and let $\alpha(f)$ be the angle between the mixing vectors $\mathbf{h}_1(f)$ of the target signal and $\mathbf{h}_2(f)$ of the jammer signal.

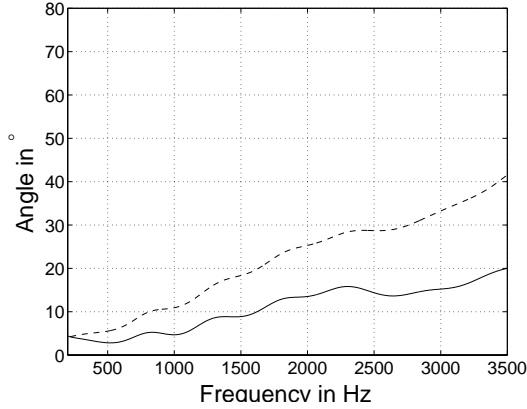
$$\mu(f) = \cos^{-1} \left(\frac{|\mathbf{h}_1^H \hat{\mathbf{h}}_1|}{|\mathbf{h}_1| |\hat{\mathbf{h}}_1|} \right) \quad \alpha(f) = \cos^{-1} \left(\frac{|\mathbf{h}_1^H \mathbf{h}_2|}{|\mathbf{h}_1| |\mathbf{h}_2|} \right) \quad (2)$$

Figure 1 shows the SVA μ for a real room (sampling rate 8 kHz, distance between microphones $d = 4$ cm, direction of arrival $\theta = 30^\circ$, FFT size: 1024). $\hat{\mathbf{h}}_1$ is approximated by $[1, \dots, e^{j2\pi \cdot (M-1)d \cdot \cos(\hat{\theta}) \frac{f}{c}}]$, and \mathbf{h}_1 is the actual impulse response measured in real environments with different reverberation times (for the database see Sec. 3.3). As seen in Fig. 1, in a reverberant environment, a much stronger SVA can occur in some frequency bins (see Fig. 1b) than the SVA caused by a rough estimation of the source position (see Fig. 1a).

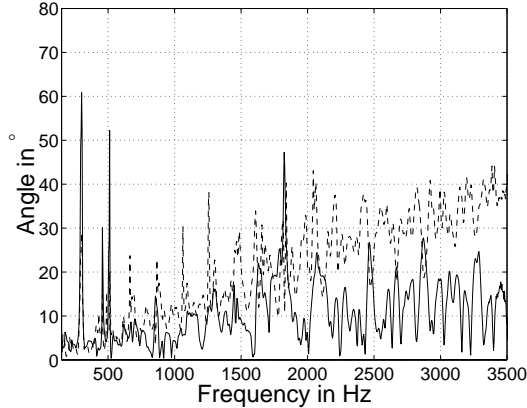
3. GEOMETRICALLY CONSTRAINED ICA

3.1. Derivation of new algorithm

The algorithm is based on negentropy maximization (3) which has been proposed by [4]. In this approach, the negentropy is approximated by the nonlinear function $G(\cdot)$ with the derivation $g(\cdot)$. As usual in ICA approaches, a PCA is applied first. Figure 2 shows a scatter plot of the sphered signals $\mathbf{z} = \mathbf{V}\mathbf{x}$. After sphering,



(a) Incorrect estimation $\Delta\theta = 20^\circ$, $T_R = 0$ ms



(b) Correct estimation $\Delta\theta = 0^\circ$, $T_R = 128$ ms

Figure 1: SVA μ induced by (a) incorrect estimation ($\Delta\theta = 20^\circ$) and (b) reverberation (solid line). The effect of reverberation exceeds the effect of an imprecise estimation. The critical angle (see Sec. 3.2) of this mixture is shown as a dashed line.

we have the following equations:

$$\arg \min_{\mathbf{t}_1} E\{G(|\mathbf{t}_1^H \mathbf{z}|^2)\} \quad (3)$$

with the constraint:

$$\mathbf{w}_1^H \hat{\mathbf{h}}_1 = \mathbf{t}_1^H \mathbf{V} \hat{\mathbf{h}}_1 = c_1 \quad (4)$$

Although most BSS algorithms claim to be unconstrained (using (3) only), they normally employ the assumption that $\mathbf{T} = [\mathbf{t}_1, \dots, \mathbf{t}_N]^H$ is unitary and, therefore, \mathbf{t}_1 has a unit length. This assumption is necessary to avoid a convergence to the point of origin and to reduce the dimensionality of the optimization problem since it can be undertaken on the unit hypersphere.

To combine BSS with the constraint, we have to weaken the assumption because a strict assumption collides with the constraint (Fig. 2). The column vectors

of \mathbf{T} need to be unitary, but they do not require a unit length. A degeneration solution is avoided by the constraint.

According to [4], the Kuhn-Tucker points of (3) are

$$E\{\mathbf{z} \cdot g(\mathbf{t}^H \mathbf{z})\} = \beta \mathbf{t} \quad (5)$$

when the derivation is performed on the unit circle $|\mathbf{t}|^2 = 1$.

We can also use this condition for points of \mathbf{t} that are not on the unit circle. If \mathbf{t} is a Kuhn-Tucker point on the unit hypersphere, then $\mathbf{t}' = \gamma \mathbf{t}$ (for any γ) is a Kuhn-Tucker point of the Lagrangian that constrains the solution to vectors of the same norm. According to the theory of FastICA, the maximal nongaussianity only says something about the direction of the unmixing vector while the norm is not decisive. We are looking for the vector that satisfies the constraint (4) and has the highest negentropy of all vectors with the same norm.

Hence, we do not change the solution of (5) by projecting it to the constraint. We obtain the following algorithm, with the convergence shown in Fig. 2.

$$\mathbf{t}^{k+1} = \mathbf{t}_k - \frac{E\{\mathbf{z}g(\mathbf{t}_k^H \mathbf{z})\} + \beta \mathbf{t}_k}{E\{\mathbf{z}g(\mathbf{t}_k^H \mathbf{z})\} + \beta} \quad (6)$$

$$\mathbf{t}^{k+1_{new}} = \frac{\mathbf{t}^{k+1}}{|\mathbf{t}_{k+1}^H \mathbf{V} \hat{\mathbf{h}}_1|} \quad (7)$$

$$\beta = \frac{E\{\mathbf{t}_k^H \mathbf{z} \cdot g(\mathbf{t}_k^H \mathbf{z})\}}{|\mathbf{t}_k|^2} \quad (8)$$

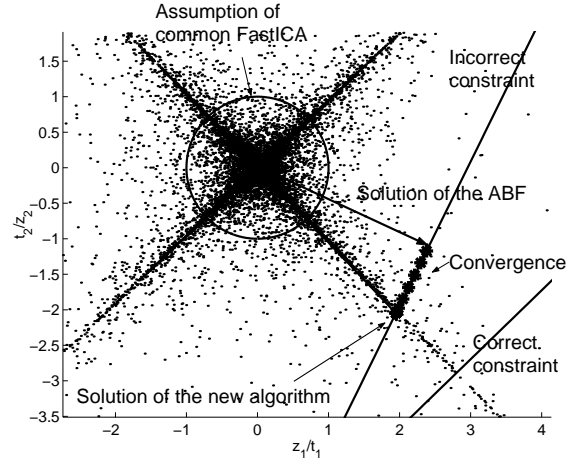
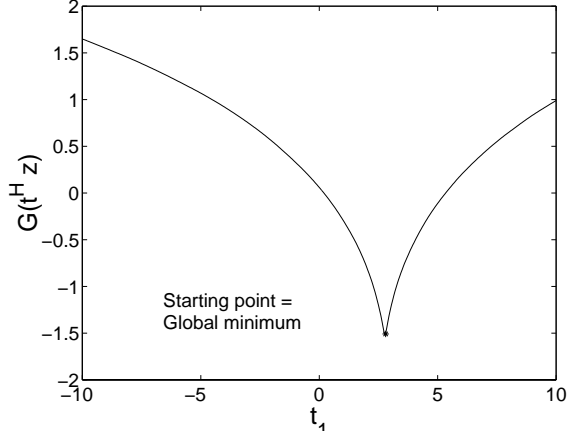
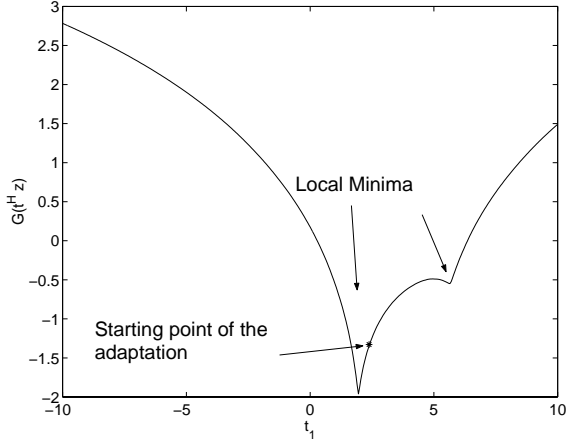


Figure 2: Convergence of the constrained FastICA algorithm. The constrained ICA algorithm starts at the solution of the ABF and converges on the constraint line to the correct solution.

The new algorithm starts with $\mathbf{t}^0 = \hat{\mathbf{t}}_1 = \mathbf{V}\hat{\mathbf{h}}_1$. If the estimation of $\hat{\mathbf{h}}_1$ is correct, the estimation itself is already the correct solution. Then, the algorithm converges according to (6)-(8) to a Lagrangian saddle point. Since the algorithm does not indicate whether it is a minimum or maximum of the cost function, an additional maximality check is introduced into the algorithm.



(a) Correct estimation, $\mu = 0^\circ$, $\alpha = 27^\circ$



(b) Incorrect estimation, $\mu = 12^\circ$, $\alpha = 27^\circ$

Figure 3: Cost function on the constraint

3.2. Theoretical assessment

The Newton method guarantees that the algorithms will converge against a Lagrangian saddle point. Figure 3(a) shows that there is only one global minimum in the case of a precise estimation of the steering vector $\hat{\mathbf{h}}_1$.

When the estimation becomes rough, two local minima and a local maximum appear (Fig. 3(b)). The two minima belong to the two signals. This means that since convergence is ensured, the algorithm converges either towards the target or the jammer. A convergence

towards the jammer signal amplifies the jammer signal and suppresses the target signal. This is equivalent to the permutation problem of the unconstrained BSS.

The shape of the Lagrangian and the starting point of the iteration control the convergence. A convergence can be guaranteed when $\hat{\mathbf{t}}_1 = \mathbf{V}\hat{\mathbf{h}}_1$ is closer to the correct solution \mathbf{t}_1 than to the permuted solution \mathbf{t}_2 because it is in the convergence range of \mathbf{t}_1 .

In the following, we derive a condition for the SVA μ and the mixing matrix that ensures that $\hat{\mathbf{t}}_1$ is close enough to \mathbf{t}_1 . Thereto, we define angles μ_{t_1} between $\hat{\mathbf{t}}_1$ and \mathbf{t}_1 and μ_{t_2} between $\hat{\mathbf{t}}_1$ and \mathbf{t}_2 ; and we restrict ourselves to $N = M = 2$ and equivalent contributions from both sources.

Let $\mathbf{R} = E\{\mathbf{x}\mathbf{x}^H\}$ be the spatial covariance matrix of the observed signals. Since it is a Hermitian matrix, it has M non zero real eigenvalues $\mathbf{\Lambda} = \text{diag}[\lambda_1, \dots, \lambda_M]$ and M orthogonal eigenvectors $\mathbf{U} = [\mathbf{u}_1, \dots, \mathbf{u}_M]$ belonging to them.

In the above defined case, \mathbf{R} has the following eigenvectors: $\mathbf{u}_1 = \frac{\mathbf{h}_1 + \mathbf{h}_2}{|\mathbf{h}_1 + \mathbf{h}_2|}$, $\lambda_1 = \sigma_s^2 \mathbf{h}_1^H (\mathbf{h}_1 + \mathbf{h}_2)$, $\mathbf{u}_2 = \frac{\mathbf{h}_1 - \mathbf{h}_2}{|\mathbf{h}_1 - \mathbf{h}_2|}$ and $\lambda_2 = \sigma_s^2 \mathbf{h}_1^H (\mathbf{h}_1 - \mathbf{h}_2)$, and the sphering matrix can be written as $\mathbf{V} = \mathbf{\Lambda}^{-1/2} \mathbf{U}$. Using the eigenvalue decomposition of \mathbf{R} , the definition of the scalar product in (2), and the angles α and μ defined in Sec. 2.2, we obtain

$$\begin{aligned} \cos(\mu_{t_1}) &= \frac{\hat{\mathbf{t}}_1^H \mathbf{t}_1}{|\hat{\mathbf{t}}_1| |\mathbf{t}_1|} = \frac{\hat{\mathbf{h}}_1^H \mathbf{V}^H \mathbf{V} \mathbf{h}_1}{|\hat{\mathbf{t}}_1| |\mathbf{t}_1|} = \frac{\hat{\mathbf{h}}_1^H \mathbf{R}^{-1} \mathbf{h}_1}{|\hat{\mathbf{t}}_1| |\mathbf{t}_1|} \\ &= \frac{\hat{\mathbf{h}}_1^H \mathbf{h}_1 + \hat{\mathbf{h}}_1^H \mathbf{h}_2}{|\hat{\mathbf{t}}_1| |\mathbf{t}_1|} + \frac{\hat{\mathbf{h}}_1^H \mathbf{h}_1 - \hat{\mathbf{h}}_1^H \mathbf{h}_2}{|\hat{\mathbf{t}}_1| |\mathbf{t}_1|} \\ &= \frac{\cos \mu - \cot \alpha \sin \mu}{|\hat{\mathbf{t}}_1| |\mathbf{t}_1|} \\ \cos(\mu_{t_2}) &= \frac{\hat{\mathbf{t}}_1^H \mathbf{t}_2}{|\hat{\mathbf{t}}_1| |\mathbf{t}_2|} = \frac{\frac{\sin \mu}{\sin \alpha}}{|\hat{\mathbf{t}}_1| |\mathbf{t}_2|} \end{aligned} \quad (9)$$

Combining the results in (9), we can define the convergence range: The algorithm will converge to the target (at least) when the miss-estimation is smaller than a critical angle μ_{critical} in (10).

$$\cot \mu < \cot \mu_{\text{critical}} = \frac{1 + \cos \alpha}{\sin \alpha} \quad (10)$$

This property is shown in Fig. 4 as a function of the SVA μ . The SIR in this figure is obtained by $20 \log[(\mathbf{w}_1^H \mathbf{H})_1 / (\mathbf{w}_1^H \mathbf{H})_2]$ for the adaptive beamformer or $20 \log[(\mathbf{W}\mathbf{H})_{11} / (\mathbf{W}\mathbf{H})_{21}]$ for the constrained ICA algorithm with a single frequency f of the Fourier transform of a real room's impulse response \mathbf{H} described in the next section. The separation performance of the adaptive beamformer decreases continuously with the

increase of the SVA, while the algorithm has a constantly good performance until the critical angle. This means that the adaptive beamformer converges correctly only when SVA is around 0° . The proposed ICA, however, converges more robustly against the wide range of SVA.

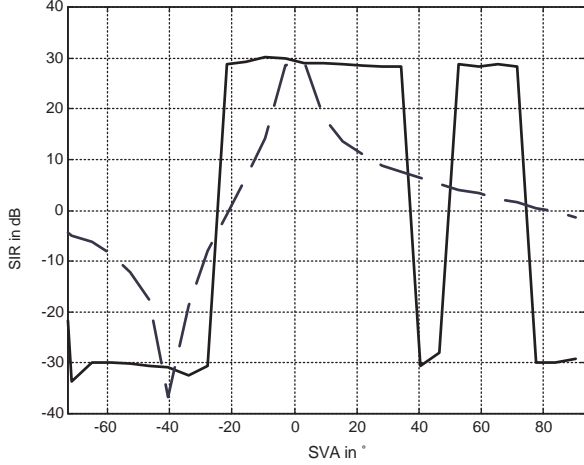


Figure 4: Comparison of the robustness of the new algorithm (solid line) and the MV beamformer (dashed line)

For a real-world acoustical application, it is important to analyze (10) with realistic numbers for the SVA μ and α in each frequency bin. Figure 1 also shows the critical angle. In both cases, the SVA μ is in almost all frequency bins under the critical angle.

3.3. Real-world assessment

We performed several tests with realistic mixtures. Japanese language sounds were mixed with room impulse responses measured in real rooms. The reverberation times were 0, 150 and 300 ms. The impulse responses where $N = M = 3$ were from the RWCP database, and a complete description is available at <http://tosa.mri.co.jp/sounddb/index.htm>. Furthermore, the algorithm has been tested with real-world mixtures for $N = M = 2$.

Figure 5 shows the signal-to-interference-ratio (SIR) in each frequency bin. The SIR is defined according to [16] and [17] as $10 \log[\sum_t y_{\text{target}}^2(t) / \sum_t y_{\text{jammer}}^2(t)]$ with y_{target} the portion of the target and $y_{\text{jammer}} = y_1 - y_{\text{target}}$ the portion of the jammer in the output signal. At almost all frequencies the algorithm converged towards the correct solution and yielded a high SIR. Negative values indicated an incorrect permutation, and this occurred mostly in the low frequency range, but also occasionally in the higher frequency

ranges. This is attributed to a large estimation error caused by the multi-path mixture and amplification by the PCA.

Incorrect steering vectors caused by (a) an incorrect look direction and (b) reverberation were used in all plots in Fig. 5. We achieved a great improvement in the frequency SIR of more than 10 dB, even in the 3×3 ($N = M = 3$) case. This demonstrates the effectiveness of the new algorithm in its major domain when a rough estimation of the steering vector is available. Although the computational cost has yet to be analyzed, the convergence is very fast due to the Newton method of the underlying FastICA algorithm.

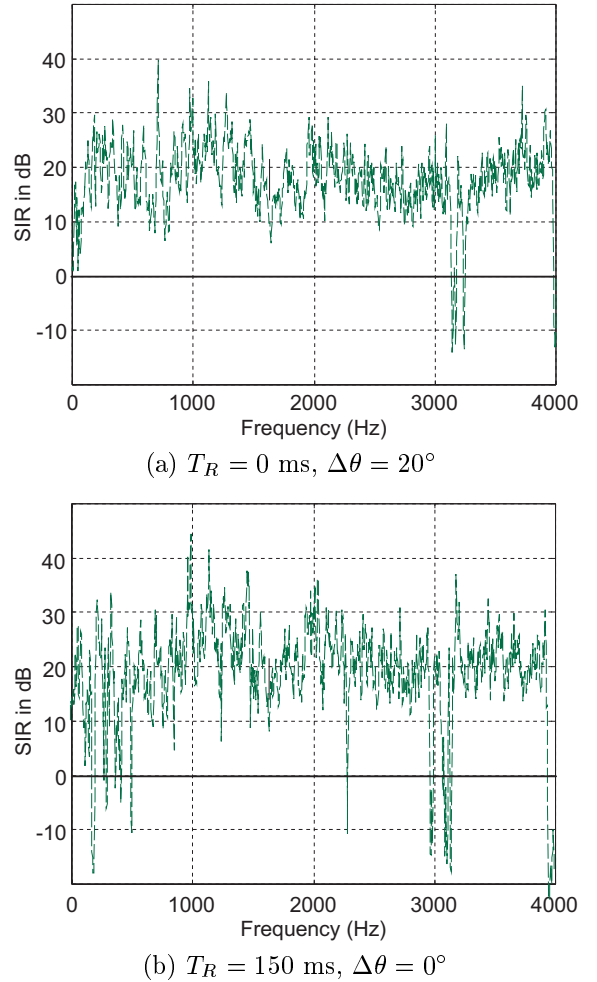


Figure 5: Real-world simulation results in $N = M = 3$

4. CONCLUSION

We introduced a new ICA algorithm with a geometrical constraint and showed its effectiveness both theoretically by defining a convergence range, and experi-

mentally by using impulse responses from a real room. The new algorithm solves the permutation problem of the BSS of acoustic mixtures, particularly when there are more than two microphones and sources.

5. ACKNOWLEDGMENTS

We thank Stefan Winter for revising the algorithms, Hiroshi Sawada and Ryo Mukai for daily cooperation and valuable discussions, and Dr. Dieter Filbert and Dr. Shigeru Katagiri for their continuous encouragement.

REFERENCES

- [1] D. Johnson and D. Dudgeon, *Array Signal Processing: Concepts and Techniques*, Prentice Hall, Englewood Cliffs, NJ, 1993.
- [2] I. Thng, A. Cantoni, and Y. H. Leung, "Constraints for maximally flat optimum broadband antenna arrays," *IEEE Trans. Signal Processing*, vol. 43, no. 6, pp. 1334–1347, June 1995.
- [3] Z. Shutao and I. Thng, "Pre-steering derivative constraint for robust broadband antenna arrays," in *ICASSP*, 2001, pp. 2913–2916.
- [4] A. Hyvärinen, J. Karhunen, and E. Oja, *Independent component analysis*, John Wiley, New York, 2001.
- [5] K. Torkkola, "Blind separation of delayed and convolved mixtures," in *Unsupervised adaptive filtering*, S. Haykin, Ed., New York, 2000, vol. 1, John Wiley.
- [6] C. Mejuto and J. Principe, "A second-order method for blind source separation of convolutive mixtures," in *Int. Conf. on BSS and ICA*, 1999, pp. 395–400.
- [7] S. Murata, S. Ikeda, and A. Ziehe, "An approach to blind source separation based on temporal structure of speech signals," Tech. Rep. 2, BSIS Riken, <http://www.bsp.brain.riken.go.jp>, 1998.
- [8] L. Parra and C. Spence, "Convolutive blind source separation of non-stationary signals," *IEEE Trans. Speech and Audio Processing*, vol. 8, pp. 320–327, 2000.
- [9] M.Z. Ikram and D.R. Morgan, "Exploring permutation inconsistency in blind separation of speech signals," in *ICASSP*, 2000, pp. 1041–1044.
- [10] S. Araki, S. Makino, R. Mukai, and H. Saruwatari, "Equivalence between frequency domain blind source separation and frequency domain adaptive null beamformers," in *Eurospeech*, 2001, pp. 2595–2598.
- [11] S. Araki, R. Mukai, S. Makino, T. Nishikawa, and H. Saruwatari, "The fundamental limitation of frequency domain blind source separation for convolutive mixtures of speech," *IEEE Trans. Speech Audio Processing* (to be published).
- [12] H. Saruwatari, S. Kurita, and T. Takeda, "Blind source separation combining frequency-domain ICA and beamforming," in *ICASSP*, 2001 pp. 2733–2736.
- [13] M. Knaak and D. Filbert, "Acoustical semi-blind source separation for machine monitoring," in *Int. Conf. on BSS and ICA*, 2001, pp. 361–366.
- [14] M. Knaak, M. Fausten, D. Filbert, "Acoustical machine monitoring using blind source separation," in *4th Int. Conf. on Acoust. and Vibratory Surveillance*, 2001, pp. 401–412.
- [15] L. Parra and C. Alvino, "Geometric source separation: Merging convolutive source separation with geometric beamforming," in *NNSP*, 2001, pp. 273–282.
- [16] R. Mukai, S. Araki, and S. Makino, "Separation and dereverberation performance of frequency domain blind source separation," in *Int. Conf. on BSS and ICA*, 2001, pp. 230–235.
- [17] H. Sawada, R. Mukai, S. Araki, and S. Makino, "Polar coordinate based nonlinear function for frequency domain blind source separation," in *ICASSP*, 2002, pp. 1001–1004.